Available online at www.sciencedirect.com
SCIENCE DIRECT
Polymer 47 (2006) 4531–4536
polymer
www.elsevier.com/locate/polymer

Direct electron paramagnetic resonance monitoring of the peptide synthesis coupling reaction in polymeric support

Clovis R. Nakaie [a,*], Luciana Malavolta [a], Shirley Schreier [b], Eliane Trovatti [c], Reinaldo Marchetto [c]

[a] Department of Biophysics, Universidade Federal de São Paulo, Rua 3 de Maio 100, CEP 04044-020 São Paulo, SP, Brazil
[b] Department of Biochemistry, Institute of Chemistry, Universidade de São Paulo, CP 26077, 05513-970 São Paulo, SP, Brazil
[c] Department of Biochemistry and Technological Chemistry, Institute of Chemistry, UNESP, Araraquara, 14800-900 São Paulo, SP, Brazil

Received 18 January 2006; received in revised form 2 May 2006; accepted 5 May 2006
Available online 22 May 2006

Abstract

This work demonstrates, for the first time, a time-resolved electron paramagnetic resonance (EPR) monitoring of a chemical reaction occurring in a polymeric structure. The progress of the coupling of a N^{α}-*tert*-butyloxycarbonyl-2,2,6,6-tetramethylpiperidine-1-oxyl-4-amino-4-carboxylic acid (Boc-TOAC) spin probe to a model peptide-resin was followed through EPR spectra. Progressive line broadening of EPR peaks was observed, indicative of an increased population of immobilized spin probe molecules attached to the solid support. The time for spectral stabilization of this process coincided with that determined in a previous coupling study, thereby validating this in situ quantitative monitoring of the reaction. In addition, the influence of polymer swelling degree and solvent viscosity, as well as of the steric hindrance within beads, on the rate of coupling reaction was also addressed. A deeper evaluation of the latter effect was possible by determining unusual polymer parameters such as the average site–site distance and site-concentration within resin beads in each solvent system.

Keywords: Peptide; Polymer; Electron paramagnetic resonance

1. Introduction

Despite the great number of studies on the subject, full understanding of the solvation characteristics of polymeric materials continues to be an elusive goal. This is attributable to the high level of complexity of the process and many approaches have been applied to investigate the influence of factor such as the resin, peptide sequence and loading and the solvent system [1–9]. In a conceptual departure from the great majority of these approaches, we have initially focused on correlating this solvation phenomenon of polymers or peptide-polymers with the media polarity. This strategy has been addressed successfully either through measurement of peptide-resin swelling in a microscope [10,11] or combined to the electron paramagnetic resonance (EPR) method, which allows the monitoring of the dynamics of the solvated polymer or peptide-polymer network [12–15] using a paramagnetic amino acid-type spin probe [16,17].

Taking into account that the presence of electrophilic and nucleophilic groups in a peptide bond (N–H and C=O moieties, respectively), might strongly affect the interaction of the peptide-resin with the solvent system, the 1:1 sum of Gutmann's [18] solvent electron acceptor number (AN) and solvent electron donor number (DN) was proposed as a dimensionless and more accurate polarity scale [10,11]. Due to the presence of opposite concepts within the same parameter, the combined polarity term (AN+DN) was adopted as the amphoteric constant [15] and used to build this alternative polarity scale. More recently, these AN and DN concepts have been also applied to aid in predicting the capacity of solvent systems, not only in terms of dissociating peptide chains attached to a polymeric structure but also free in solution [19].

As a natural continuation of this effort to introduce as much variance as possible into the investigation of polymer solvation characteristics, the present study aimed to carry out, for the first time, a real-time monitoring of the coupling reaction within a resin. However, the acylating component for this reaction of binding to the solid support was the spectral probe molecule itself, which will allow in situ monitoring of this coupling

* Corresponding author. Tel.: +55 11 5539 0809; fax: +55 11 5575 9617.
E-mail address: clovis@biofis.epm.br (C.R. Nakaie).

0032-3861/$ - see front matter © 2006 Elsevier Ltd. All rights reserved.
doi:10.1016/j.polymer.2006.05.007

time-resolved experiment. The N^{α}-*tert*-butyloxycarbonyl (Boc)-2,2,6,6-tetramethylpiperidine-1-oxyl-4-amino-4-carboxylic acid (TOAC) amino acid-type paramagnetic probe (Boc-TOAC) [16] was coupled to a model peptide resin, and the progress of this acylation reaction to the polymer backbone was monitored directly by electron paramagnetic resonance (EPR) spectroscopy. In addition, the influence of the degree of peptide-resin swelling, media viscosity and degree of peptide-chain steric hindrance within beads were also examined in this coupling kinetics approach.

2. Experimental

2.1. Materials

Reagents and solvents were of analytical grade, were collected from recently opened containers and were not further purified. The styrene–1% divinylbenzene copolymer attaching phenylmethylamino groups and denoted benzhydrylamino-resin (BHAR) [20] was selected for peptide chain assembly.

2.2. Methods

2.2.1. Peptide synthesis

The (Asn-Ala-Asn-Pro) sequence was synthesized manually by standard Boc-chemistry [21,22] on about 0.5 g of 0.14 and 1.4 mmol/g BHAR. Coupling was performed using a 2.5 excess of Boc-amino acid/DIC/HOBt (1:1:1) in DCM/DMF for approximately 2 h. All couplings were monitored by qualitative ninhydrin test and, when positive, acetylation was performed with 50% acetic anhydride in DCM for 15 min.

2.2.2. Measurement of peptide-resin swelling

Before swelling measurement of resins, all batches of synthesized peptide-BHARs were sized by suspension in ethanol and fine materials were decanted off. The suspension was allowed to stand until approximately 90–95% had settled before decanting the supernatant. This procedure was repeated five times and was followed by suspending the beads in DCM and, solvent containing fine particles was withdrawn. This was also repeated about five times. In order to develop the swelling study with as narrowly sized population of beads as possible, the last purification step of resins involved repeated sifting of dry beads through several 44–88 μm pore metal sieves. This sieving procedure lowered the standard deviation of the resin diameters to about 4%.

Swelling studies of the small-diameter bead populations were performed as published elsewhere [1,10,15] after the resins were dried in vacuum using an Abderhalden-type apparatus. About 200 dry and swollen (allowed to solvate overnight) beads from each resin were spread over a microscope slide and measured directly with a microscope coupled with Image-Pro Plus software. The values of bead diameter distribution were estimated by the geometric means and geometric standard deviations.

2.2.3. EPR studies

EPR measurements were carried out at 9.5 GHz in an EPR spectrometer at room temperature (22 ± 2 °C) using flat quartz cells. Labeled peptide resins were pre-swollen overnight in the solvent under study. The magnetic field was modulated with amplitudes less than one-fifth of the line-widths, and the microwave power was 5 mW to avoid saturation effects. Details of TOAC derivative-labeling of resins have been already reported [12–15].

2.2.4. Yield of the coupling reaction

In a reaction vessel thermostated at 25 °C, 50–100 μmol of peptide-BHAR were equilibrated with the desired solvent. Pre-formed symmetrical anhydride (PSA) of the Boc-TOAC was produced by mixing with DCC in equimolar conditions (for 1 h, at 0 °C). The white precipitate was removed by filtration and the solution was evaporated for further dissolution with the desired solvent for comparative coupling experiments. The PSA method was deliberately chosen for these experiments as it is less susceptible to the effect of the polarity of the solvent [21,22]. The rate of rotation of the reaction flask was 20 rpm. The acylating reagents were dissolved in the solvent under investigation and added in equimolar condition (at 10^{-2} M concentration of reactants) to the reaction vessel, containing peptide resin pre-swollen in the same solvent. The yield of coupling was monitored by the picric acid method [23], and each experiment was performed in duplicate.

3. Results and discussion

Table 1 displays the swelling degrees and the kinetics of the coupling reactions of Boc-TOAC in two $(NANP)_4$–BHAR

Table 1
Correlation between Boc-TOAC coupling yield to $(NANP)_4$–BHAR in different solvents and swelling parameters

Solvent	$(NANP)_4$–BHAR[a]				$(NANP)_4$–BHAR[b]			
	Volume solvent/bead (10^4 μm^3)[c]	Coupling yield (%)			Volume solvent/bead (10^4 μm^3)[c]	Coupling yield (%)		
		30 min	60 min	180 min		30 min	60 min	180 min
DCM	17	54	61	78	12	24	50	74
DMF	28	83	88	93	53	43	82	92
DMSO	17	33	46	65	96	80	87	89

Yield of Boc-TOAC coupling at 25 °C with preformed symmetrical anhydride method in equimolar conditions (2 mM concentration of reactants).
[a] Obtained from a 0.14 mmol/g BHAR.
[b] Obtained from a 1.40 mmol/g BHAR.
[c] Volume of swollen bead − volume of dry bead.

Table 2
Swelling parameters of differently labeled Boc-TOAC–$(NANP)_4$–BHAR in DCM

Sample	Col. 1	Col. 2	Col. 3	Col. 4	Col. 5	Col. 6	Col. 7	Col.8	Col. 9	Col 10
Resin (mmol/g)[a]	Diam. dry bead (μm)	Diam. swollen bead (μm)	Volume solvent/ bead (10^5 μm^3)	Volume dry sample/g copol. (mL)[b]	Weight dry sample/g copol. (g)	Volume dry sample/g sample (mL)	Number of beads/g sample (10^7)	Number of sites/bead (10^{12})	Site–site distance (Å)	Site conc. (M)
0.111[c]	61	82	1.7	2.2	1.48	1.49	1.25	7.0	34.5	0.068
0.385[d]	68	82	1.2	3.1	4.26	0.72	0.44	52.6	17.6	0.730

Calculated according to Ref. [25].
[a] Degree of Boc-TOAC labelling.
[b] Copolymer of styrene–1% divinylbenzene: $d=0.99$ g/mL; average diameter of dry beads $=47$ μm.
[c] Obtained from a 0.14 mmol/g BHAR.
[d] Obtained from a 1.40 mmol/g BHAR.

batches in DCM, DMF and DMSO. The substitution degrees of both solid supports were 0.14 and 1.4 mmol/g, respectively, which allowed final peptide loadings of 14 and 68% (weight/weight). The resin-bound tetradecapeptide sequence corresponds to the antigenic and immunodominant segment of the sporozoite form of *Plasmodium falciparum* involved in malaria transmission [24]. To facilitate the determination of coupling yield, unfavorable experimental conditions were deliberately created, with a low reactant concentration (0.002 M) that was in equimolar proportion with the amount of the amino-group component of the peptide-resin.

The yield of coupling reactions was directly related to the degree of swelling, regardless of the peptide-resin involved (Table 1). Accordingly, DMF and DMSO allowed faster acylation for the lightly- and heavily-peptide-loaded resins, respectively. However, when the swelling degrees were equivalent, as in the case of the lightly- (14%)-peptide-loaded BHAR in DCM and DMSO (1.7×10^5 μm^3 of solvent volume absorbed per bead), the acylation was faster in the less viscous solvent (DCM). This finding indicates that the difference in viscosity between the two solvents (0.4 and 2.0 Cp, respectively), clearly affects the coupling reaction rate, even within the polymer matrix.

In addition to swelling degree and viscosity, the third factor influencing the coupling reaction is the steric hindrance degree within beads, as previously mentioned. The effect of this factor can be seen for example, when the coupling yield of both peptide-resins in DMF is compared (Table 1). The coupling rate of the highly (68%) peptide-loaded resin is slower, although presenting greater swelling than its low (14%) peptide-loaded partner resin (5.3×10^5 and 2.8×10^5 μm^3, respectively).

By considering these swelling values and the degree of substitution of resins and the molecular weight of attached peptides, it was possible to estimate the average distance between peptide chains spread throughout the bead matrices in both peptide-resins, according to our recently published report [25]. Tables 2 and 3 display the calculated values found for the low and highly peptide-loaded resins of Table 1 in DCM and DMF, respectively. In order to detail how the various peptide-resins parameters were sequentially calculated, the detailed procedure will be next described for the 0.111 mmol/g Boc-TOAC–$(NANP)_4$–BHAR batch in DMC (Table 2, row 1).

3.1. Example: 0.111 mmol/g labeled Boc-TOAC–$(NANP)_4$–BHAR swollen in DCM (Table 2)

Columns 1 and 2 list the average diameters of the dry (61 μm) and DCM swollen (82 μm) beads, respectively, measured under the light microscope. The volumes of the dry (1.19×10^5 μm^3) and swollen (2.89×10^5 μm^3) beads were calculated and the volume of solvent/bead (1.7×10^5 μm^3, column 3) was obtained by subtracting the dry bead volume from the swollen bead volume.

Table 3
Swelling parameters of differently labeled Boc-TOAC–$(NANP)_4$–BHAR in DMF

Sample	Col. 1	Col. 2	Col. 3	Col. 4	Col. 5	Col. 6	Col. 7	Col.8	Col. 9	Col 10
Resin (mmol/g)[a]	Diam. dry bead (μm)	Diam. swollen bead (μm)	Volume solvent/ bead (10^5 μm^3)	Volume dry sample/ g copol. (mL)[b]	Weight dry sample/g copol. (g)	Volume dry sample/g sample (mL)	Number of beads/g sample (10^7)	Number of sites/ bead (10^{12})	Site–site distance (Å)	Site conc. (M)
0.111[c]	61	91	2.8	2.2	1.48	1.49	1.25	7.0	38.3	0.042
0.385[d]	68	110	5.3	3.1	4.26	0.72	0.44	52.6	23.7	0.165

Calculated according to Ref. [25].
[a] Degree of Boc-TOAC labeling.
[b] Copolymer of styrene–1% divinylbenzene: $d=0.99$ g/mL; average diameter of dry beads $=47$ μm.
[c] Obtained from a 0.14 mmol/g BHAR.
[d] Obtained from a 1.40 mmol/g BHAR.

3.2. Column 4: volume of dry sample/g of copolymer (2.2 mL/g copolymer)

The ratio (diameter dry sample/diameter dry copolymer)^3 represents the relationship between the volume of the dry macroscopic working sample (0.111 mmol/g Boc-TOAC–$(NANP)_4$–BHAR) and that of the dry copolymer used to synthesize the sample. In the example, since the average diameters of beads of dry sample and dry copolymer are 61 and 47 μm, respectively, the ratio between the dry volumes of both resins is $(61/47)^3=2.18$. Considering that the number of beads in 1 g of copolymer is the same as in the sample synthesized from this amount of copolymer and taking into account that the volume of 1 g of copolymer is 1.01 mL ($d=0.99$ g/mL), the total volume of dry sample containing 1 g of copolymer is therefore 2.18×1.01 mL, or 2.20 mL.

3.3. Column 5: weight of dry sample/g of copolymer (1.48 g/g of copolymer)

The 0.111 mmol Boc-TOAC–$(NANP)_4$–BHAR sample was synthesized by quantitative incorporation of the $(NANP)_4$ peptide and Boc-TOAC in the 0.140 mmol/g BHAR batch. This resin originated from partial phenylmethylamino incorporation into a heavily substituted 1.40 mmol/g benzoyl group-containing copolymer. This copolymer derivative is synthesized in the first step (Friedel–Crafts acylation) necessary to obtain BHAR. Thus, the Boc-TOAC–$(NANP)_4$–BHAR sample under consideration still contains (1.40–0.14) mmol = 1.26 mmol/g of remaining benzoyl groups attached to its backbone. Considering the total weight of groups added in all the synthetic steps, one can calculate that the sum of Boc-TOAC, $(NANP)_4$ peptide and benzoyl groups attached to the initial copolymer corresponds to 0.325 g. Therefore, in 1 g of sample, the mass of copolymer is $1-0.409$ g $=0.675$ g. Thus, for 1 g of starting copolymer, the weight of the 0.111 mmol Boc-TOAC–$(NANP)_4$–BHAR is 1.48 g.

3.4. Column 6: volume of dry sample/g of sample (1.49 mL/g)

This parameter is calculated by dividing the value of (volume of dry sample/g copolymer), column 4, by (weight of dry sample/g copolymer), column 5. The value obtained (1.49 mL/g) represents the ratio between the volume of the dry sample (2.2 mL) and its total weight (1.48 g), and corresponds to the volume occupied by 1 g of sample in the dry form.

3.5. Column 7: number of beads/g of sample (1.25×10^7 beads/g sample)

This value is calculated by dividing the volume of 1 g of dry sample (1.49 mL, column 6) by the average volume of one dry bead, which is calculated from its diameter (61 μm, column 1). Thus, the volume of one dry bead is 1.19×10^{-7} mL. The ratio 1.49 mL/1.19×10^{-7} mL yields 1.25×10^7 beads in 1 g of sample.

3.6. Column 8: number of sites/bead (7.0×10^{12})

The number of sites per bead is calculated by dividing the number of sites/g of sample by the number of beads/g of sample (column 7). The former value corresponds to $0.145\times6.02\times10^{20}$ sites/g. Dividing this number by the number of beads in 1 g of sample (1.15×10^{7}, column 7) one obtains 7.0×10^{12} sites/bead.

3.7. Column 9: site–site distance (34.5 Å).

To evaluate this important parameter, we first calculate the average volume per site. This is done by dividing the volume of one swollen bead (2.89×10^{5} μm^3, calculated from the measured diameter of one swollen bead, 82 μm, column 2) by the number of sites/bead (7.0×10^{12}, column 8). Thus, the average volume per site is 4.1×10^{4} Å^3. By assuming a uniformly distributed cubic lattice for the sites within the bead, the site–site distance corresponds to the side of a cube and is given by the cubic root of the volume occupied by one site, i.e. $(4.1\times10^{4}\ \text{Å}^3)^{1/3}=34.5$ Å.

3.8. Column 10: site concentration inside the bead (0.068 mM).

Finally, making use of the parameters calculated in the previous steps, it is possible to determine the site concentration within the bead. Thus, for the 0.145 mmol/g substituted Boc-TOAC–$(NANP)_4$–BHAR, the site concentration is obtained by dividing the number of sites/bead (7.0×10^{12}, column 8) by the volume of solvent/bead (1.7×10^{5} μm^3, column 3), that is, 4.1×10^{7} sites/μm^3, or 4.1×10^{19} sites/mL. Considering that 6.02×10^{20} sites/mL correspond to 1 M concentration, we find that that the site concentration corresponds to an effective Boc-TOAC concentration of 0.068 mM.

Using this calculation strategy also for other data shown either in Tables 2 and 3, it was possible for instance to seen that the average inter-site distance values of 34.5 and 17.6 Å in DCM (Table 2) and 38.3 and 23.7 Å in DMF (Table 3) were determined for these two peptide-bound resins, respectively. In addition, the effective peptide chain concentrations inside the bead were also determined giving the values of 0.068 and 0.730 M in DCM (Table 2) and 0.042 and 0,165 M in DMF (Table 3), respectively. Thus, regardless the peptide-resin, the greater the distance between reactive sites, the faster is the coupling reaction. Taken together, these findings therefore proves clearly the influence of the level of the steric hindrance in neighbouring peptide chains, decreasing the rate of reaction as a consequence of the greater proximity between the chains under conditions of heavier peptide loading.

Following these results, the direct EPR monitoring of the Boc-TOAC spin probe coupling reaction in the $(NANP)_4$–BHAR (1.4 mmol/g) was next tested in DMF, using the same acylation protocol employed for the experiments detailed in Table 1. Fig. 1 reveals a clear line broadening of EPR spectral peaks over the course of the coupling reaction. This line broadening was induced by the increasing immobilization of

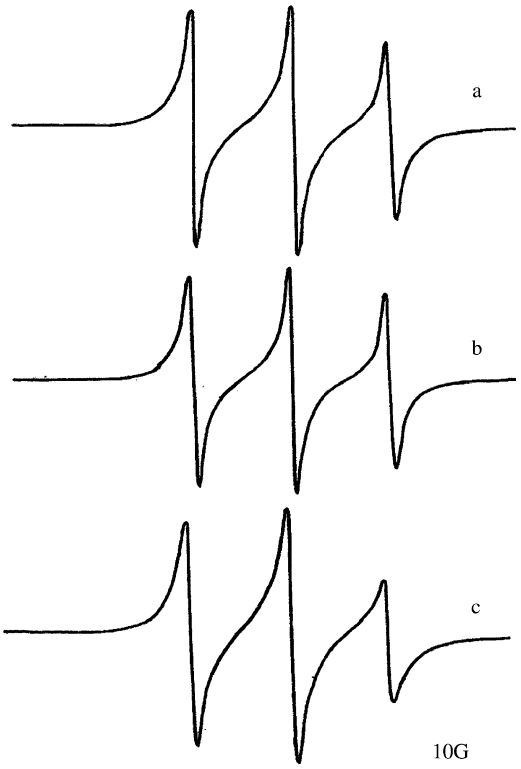

Fig. 1. EPR spectra of Boc-TOAC coupling in $(NANP)_4$–BHAR (1.4 mmol/g) after (a) 0, (b) 60 and (c) 180 min. Reaction at 25 °C in DMF, with preformed symmetrical anhydride method in equimolar conditions and 2 mM concentration of reactants.

the Boc-TOAC molecule population attached to the polymer backbone.

Although most of biradicals known in the literature display a five-line pattern in the EPR spectra, the biradical formed for coupling to resin matrix and corresponding to the reactive symmetrical anhydride of the Boc-TOAC probe gives a three line-type spectrum as can be seen in Fig. 1(a). This result seems to be in accord with the observation that the structure and the average distance between both nitroxide moiety in the biradical

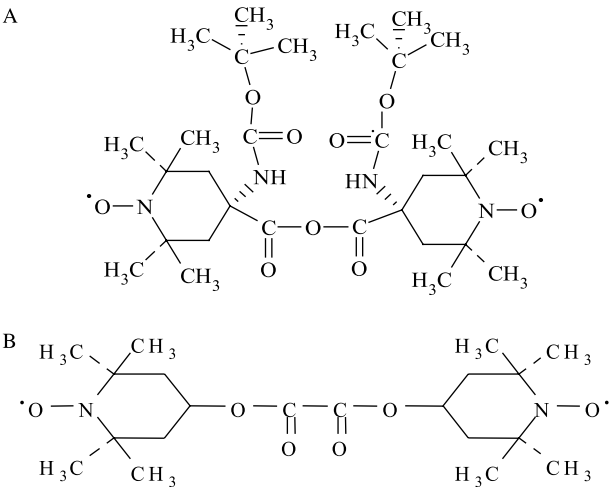

Fig. 2. Molecular structures of the biradicals (A), symmetrical anhydride of N^{α}-*tert*-butyloxycarbonyl-2,2,6,6-tetramethylpiperidine 1-oxyl-4-amino-4-carboxylic acid and (B), bis(2,2,6,6-tetramethylpiperidine-1-oxyl) oxalate.

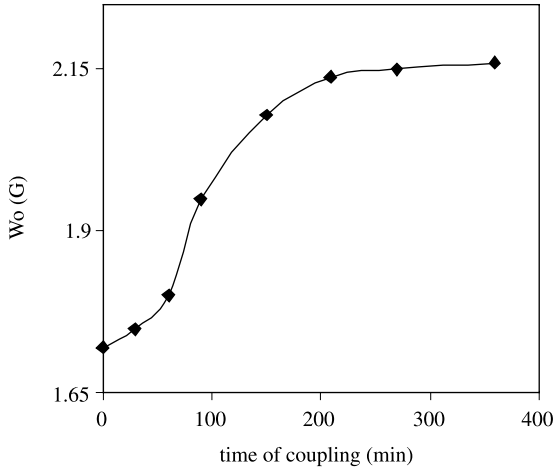

Fig. 3. Correlation between EPR central Wo linewidth values and time of Boc-TOAC coupling to $(NANP)_4$–BHAR (1.4 mmol/g). The reactions were carried out at 25 °C in DMF, with preformed symmetrical anhydride method in equimolar conditions, and 2 mM concentration of reactants.

molecule may affect the EPR spectrum profile [26–28]. To better clarify this issue, the Fig. 2 shows the similarity existing between the structure of Boc-TOAC symmetrical anhydride and that of the bis(2,2,6,6,-tetramethylpiperidine-1-oxyl) oxalate paramagnetic probe. According to the literature, this latter biradical also displays a three line-type EPR spectrum [28].

Next, Fig. 3 shows the correlation between line-width values of the middle-field EPR peak (Wo) and reaction times. This EPR parameter has been often used for determination of the degree of motion of labeled molecules or systems [12–15,25]. As can be seen in the figure, progressive increase in the line-width values of peaks followed by complete stabilization of Wo values (greater immobilization) occurred after 3–4 h of coupling, thus in agreement with data shown in Table 1. These findings therefore, demonstrate the feasibility of carrying out direct, in situ monitoring of a chemical reaction within the polymer structure in which the reacting component is the spectral probe itself.

In summary, our results seem to be of value for increasing the understanding of the solvation characteristics of polymers. We have demonstrated that various physicochemical and structural factors influence the reaction yield in polymers. However, the innovative aspect of the present report is the finding that the EPR approach allows direct time-resolved monitoring of a specific chemical reaction (coupling) occurring throughout the polymer network. The success of this experimental strategy might be of relevance in devising other approaches intended to further investigate, at the microenvironment level, chemical processes in polymers.

Acknowledgements

We gratefully acknowledge FAPESP, CNPq, CAPES and FADA for financial support. All authors are recipients of research fellowships from CNPq.

References

[1] Sarin VK, Kent SBH, Merrifield RB. J Am Chem Soc 1980;102:5463–70.
[2] Fields GB, Fields CG. J Am Chem Soc 1991;113:4202–7.
[3] Kates SA, Albericio F. Solid phase synthesis: a practical guide. New York: Marcel Dekker, Inc.; 2000 p. 275–330.
[4] Vaino AR, Janda KD. J Comb Chem 2000;2:579–96.
[5] Deber CM, Lutek MK, Heimer EP, Felix AM. Peptide Res 1989;2:184–8.
[6] Furrer J, Piotto M, Bourdonneau M, Limal D, Guichard G, Elbayed K, et al. J Am Chem Soc 2001;123:4130–8.
[7] Warrass R, Wieruszeski M, Bouitillon C, Lippens G. J Am Chem Soc 2000;122:1789–95.
[8] Valente AP, Almeida FCL, Nakaie CR, Schreier S, Crusco E, Cilli EM. J Pept Sci 2005;11:556–63.
[9] Yan B. Acc Chem Res 1998;31:621–30.
[10] Cilli EM, Oliveira E, Marchetto R, Nakaie CR. J Org Chem 1996;61: 8992–9000.
[11] Malavolta L, Oliveira E, Cilli EM, Nakaie CR. Tetrahedron 2002;58: 4383–94.
[12] Cilli EM, Marchetto R, Schreier S, Nakaie CR. Tetrahedron Lett 1997;38: 517–20.
[13] Cilli EM, Marchetto R, Schreier S, Nakaie CR. J Org Chem 1999;64: 9118–23.
[14] Ribeiro SCF, Schreier S, Nakaie CR, Cilli EM. Tetrahedron Lett 2001;42: 3243–6.
[15] Oliveira E, Cilli EM, Miranda A, Jubilut GN, Albericio A, Andreu A, et al. Eur J Org Chem 2002;21:3686–94.
[16] Nakaie CR, Schreier S, Paiva ACM. Braz J Med Biol Res 1981;14: 173–80.
[17] Marchetto R, Schreier S, Nakaie CR. J Am Chem Soc 1993;15: 11042–3.
[18] Gutmann V. The donor–acceptor approach to molecular interactions. New York: Plenum Press; 1978.
[19] Malavolta L, Nakaie CR. Tetrahedron 2004;60:9417–24.
[20] Pietta PG, Cavallo PF, Takahashi K, Marshall GR. J Org Chem 1974;39: 44–8.
[21] Barany G, Merrifield RB. The peptides, vol. 2. New York: Academic Press; 1979 p. 1–284.
[22] Stewart JM, Young JD. Solid phase peptide synthesis. Rockford III: Pierce Chemical Company; 1984.
[23] Gisin BF. Anal Chim Acta 1972;60:248–9.
[24] Dame JB, Williams JL, McCutchan TF, Weber JL, Wirtz RA, Hockmeyer WT, et al. Science 1984;225:593–9.
[25] Marchetto R, Cilli EM, Jubilut GN, Schreie S, Nakaie CR. J Org Chem 2005;70:4561–8.
[26] Calvin M, Wang HH, Entine G, Gill D, Ferruti P, Harpold MA, et al. Proc Natl Acad Sci, USA 1969;63:1–8.
[27] Sankarapandi S, Sukumar M, Balaram P, Manoharan PT. Biochim Biophys Res Commun 1995;213:439–46.
[28] Rozantsev EG. In: Ulrich H, editor. Free radicals. New York: Plenum Press; 1970.